Shock Waves (2012) 22:615–625
DOI 10.1007/s00193-012-0396-5

ORIGINAL ARTICLE

Studies of DDT enhancement approaches for kerosene-fueled small-scale pulse detonation engines applications

Y. Huang · H. Tang · J. Li · C. Zhang

Received: 13 June 2011 / Revised: 6 October 2011 / Accepted: 12 May 2012 / Published online: 10 July 2012

Abstract Two-phase small-scale pulse detonation engine (SPDE) offers a competitive alternative for small-scale propulsion systems from a high cycle efficiency and structural simplicity standpoint. SPDE models are designed with the aero-valve, and three different cases of obstacle combinations are used as deflagration-to-detonation transition (DDT) devices. The inner diameters of detonation tubes are 29 mm, and the lengths of three SPDEs are 995, 1,100, and 1,175 mm. Using kerosene-air as the fuel-oxidizer, a series of high-frequency detonation tests is conducted to seek efficient DDT enhancement approaches that reduce DDT distance and time and increase the frequency of kerosene-fueled SPDE. The results show that the fully developed detonation wave can be achieved at a distance of 3.4 times the minimum characteristic distance for gaseous detonation formation from the igniter and that the SPDE can steadily operate at a maximal frequency of 62.5 Hz. By adopting these DDT enhancement approaches, the detonability of kerosene is significantly improved. In addition, experiments are performed to study the effects of firing frequencies on detonation transitions. The results clearly indicate that the values of detonation wave pressures and velocities, the degree of overdriven wave, the ignition delay times, and detonation initiation times vary with frequencies. In terms of the performance, the optimal frequencies of three SPDE models are 20, 42.5, and 50 Hz, respectively.

Communicated by F. Lu.

Y. Huang (✉) · H. Tang · J. Li · C. Zhang
Nanjing University of Aeronautics and Astronautics,
Nanjing 210016, Jiangsu, China
e-mail: huangyue2010@gmail.com

Keywords Deflagration-to-detonation transition · High frequency · Kerosene · Pulsed detonation engine · Small-scale propulsion system

1 Introduction

A pulse detonation engine (PDE) is a new unsteady propulsion device that produces thrust by burning out fuel to initiate repeated propagating detonation waves [1]. Because of high efficiency of the detonation cycle and its simple structure, PDEs can offer better performance compared with conventional propulsion devices. Recently, small-scale or micro-PDE technology has attracted considerable attention because of their potential advantages and the growing interests in the use of micro-propulsion systems. McManus et al. [2] mentioned a small propulsion system based on PDE, and Kitano et al. [3] summarized variable applications of the small size or micro-PDE including satellite altitude control, micro power generation application similar to micro gas-turbine generator, compact detonation spraying system, and pre-detonation initiator. Both studies were limited to gaseous fueled operations. Therefore, from a practical perspective, it is possible to create a new feasibility for the design of small-scale propulsion systems using detonation model of liquid kerosene. According to the recent studies on the PDE, a liquid-fueled small-scale PDE (SPDE) was defined as that whose diameter was less than 30 mm and the overall length was less than 1.5 m [4].

Under certain conditions, a deflagration wave may spontaneously accelerate and trigger an explosion in the mixture undergoing transition to a detonation wave [5]. This process is often referred to as deflagration-to-detonation transition (DDT) [6]. The study of DDT has showed that there are numerous DDT scenarios and all the details of DDT

process cannot be reproduced in experiment [7]. Theoretical and experimental investigations of DDT were successfully used for evaluating PDEs and developing prototypes [8]. Although some significant insights have been obtained through many excellent experimental as well as theoretical studies, achieving DDT remains one of the major challenges of the PDE [9], especially in two-phase detonation. Thus, achieving a stable and fast onset of detonation in the two-phase mixture using the adaptable DDT enhancement approaches is one of key factors characterizing the PDE.

To optimize PDE performance and enable high operating frequencies, reduction of the DDT run-up distance is required. The DDT can be promoted by incorporating larger-diameter cavities in the ignition section [10–12];inserting regular or irregular obstacles (such as Shchelkin spiral, orifice plates, shock-focusing end-walls) [13–18]; and introducing the Shchelkin spiral in the ignition section [19], and these effective measures worked by affecting the rate of flame acceleration. Most of the previous studies adopted gaseous fuel in the experiments [13]. Due to the low reactivity of two-phase fuel-air mixtures, very few works have been conducted on fast deflagration and detonation of two-phase mixture. However, various attempts have been made to investigate the DDT of two-phase mixtures. The results of theoretical and experimental investigations of the detonation initiation in heterogeneous polydispersed mixtures of hydrocarbon fuels with air have been presented by Smirnov et al. [12]. A static reverse valve was used to make the pulse detonation device (the tube diameter was 80 mm and tube length was 2,000 mm) highly reliable; the effective measures including wider cavities in the ignition section and preheating of fuel were adopted to bring a stable periodical onset of detonation in the frequencies of 5–10 Hz. In order to obtain full developed detonation of a kerosene–air mixture at the shortest distances and the minimal ignition energies, some DDT enhancement approaches were used to speed up the detonation transition by Frolov et al. [16–18]. These approaches included application of a pre-detonator with a high reactivity fuel–oxygen mixture, the measures to improve fuel detonability, flame acceleration by means of regular obstacles, and multiple reflections of the generated shock wave in a special focusing device and a coil. In their experiment, the inner diameter of detonation tube was 52 mm and the total length of PDE was 3 m. The detonation waves were successfully produced in the single-shot tests and in the low-frequency multi-cycle tests (maximal frequency at 8 Hz). Nevertheless, detonation in a SPDE at high frequency could be significantly different with previous studies in the single-shot and the low-frequency tests. Furthermore, the decreases in the diameter and in the length of detonation tube will make an important impact on the detonation transition. Hence, for utilizing the kerosene as the potential fuel and optimizing the performance, there is a further need to understand DDT in the multi-cycle SPDE systems using these approaches at the high frequencies.

To microminiaturize the PDE, DDT enhancement approaches should be efficient enough to attain successful detonation in the tube with smaller diameter and shorter length. Thus, it is important to improve understanding how these geometries interact with the flame and shock to produce ample conditions of DDT in the above approaches.

In the present study, liquid aviation kerosene and air are used as the fuel and the oxidizer. To seek efficient DDT enhancement approaches, a series of multi-cycle detonation experiments is carried out with low ignition energies. DDT enhancement approaches are adopted in the tests, including the enhancement of fuel detonability, flame acceleration by regular obstacles (Shchelkin spiral and orifice plates), and multiple reflections of the generated shock wave in a special focusing device (shock-focusing end-walls). Three different combinations of obstacles are used as DDT devices in these SPDE models, and the run-up distance and the propagating characteristics of the DDT process are determined. Besides, experiments are performed to investigate the effects of firing frequency on detonation transitions. The optimal frequencies of SPDE models are determined as well.

2 Experimental setup

The experimental facility and instrumentation are illustrated in Fig. 1, and the main composed parts of the experimental system are the fuel and air supply system, the control system, the data acquisition system, the test stand, and the SPDE model. The SPDE model is composed of several major detachable sections such as aero-valve, the premixed section, the ignition section, the DDT enhancements section, and the detonation “blow-down” section.

There are many physical methods to speed up DDT in fuel–air mixtures, namely, obstacle-forced flame acceleration, shock reflections and focusing, resonant amplification of shocks by traveling ignition pulses, and various devices applying the combinations of the approaches listed [13]. To study the effects of internal geometry on DDT, two different obstacle geometries and a shock-focusing end-wall are designed as showed in Fig. 2, and all blockage ratios (BR) were 0.43.

The larger-diameter cavity is used as an ignition section in the experiments; the “Simirnov’s cavities” have been proven as an effective measure for achieving DDT [10–12]. An electric ignition rod is located at a distance of 220 mm from the outlet of aero-valve. To improve ignition reliability, the flame is anchored on a v-type bluff-body flame holder, having a parabolic cross section (had a width of 16 mm and a blocking ratio of 12 %), located 20 mm upstream of the ignition point. The schematic illustration of ignition section and flow

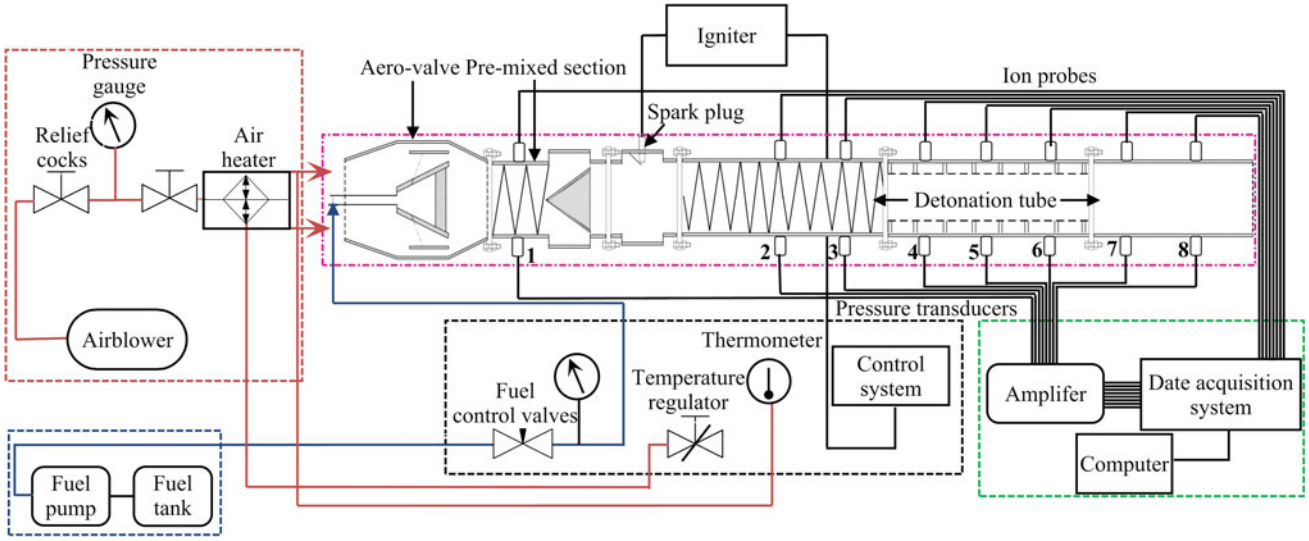

Fig. 1 Experimental facility and instrumentation

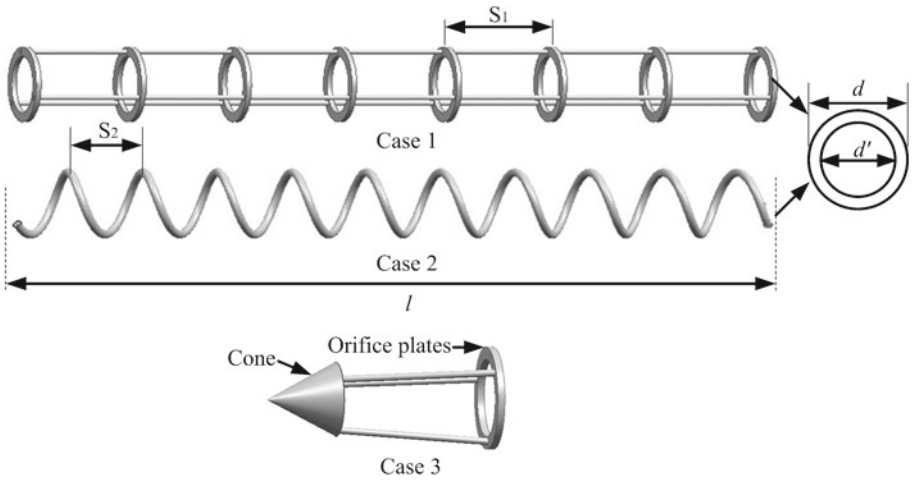

Fig. 2 DDT obstacle geometries

distribution of v-type bluff-body flame holder was described in detail in the work of Huang et al. [4,20]. The maximum effective discharge energy is estimated to be 0.5 J and the discharge current duration through the igniter is 40 ± 5 μs. The ignition frequency is controlled by a self-developed automotive control module. The data acquisition system consists of two National Instruments S series PXI 6115 modules (4 Channel, maximum sampling rate of 2.5 MSa/s per channel) housed in a 1042-Q chassis. The pressure transducers and ion probes are connected to the data acquisition system through a Signal Conditioner module, and then the signals are transformed into data by PC. The transducers and ion probes are sampled at 0.4 MSa/s for 20 s per run. This fast sampling rate is adopted to resolve accurately the high-speed transient events during the operating cycle.

Liquid kerosene is injected through the small tangential oil holes which distribute around the oil cavity surface of the aero-valve, producing a mist of oil. The emission of oil mist on the oil ring is further atomized with the high-velocity airflow from both sides of the throat. Air for the SPDE is supplied with the low-head Roots Blower. The mass flow of both air and liquid kerosene are controlled by the mechanical screw to keep the fuel-air ratio approximately equal to the constant equivalent ratios that produce the high-quality detonable mixture during an experimental run. Due to the low reactivity of jet kerosene–air mixtures, some measures are taken to improve the detonability of mixture by preheating the fuel and enhancing the fuel-air premixing. Results of the experimental debugging demonstrate that these measures reduce both detonation initiation energy and DDT time. The pretreatment system consists of an air heater and a premixed section. The initial temperature of air is 25 °C and the temperature of preheated kerosene is 110 °C.

3 Presentation of results

In the DDT, the penalizing mechanism is the production of turbulence during the long run-up of the flame prior to DDT [18]. In order to shorten the DDT distance, a rapid increase of turbulence and gradients in the mixture is necessary. The flames pass through the obstacles to stretch flame surfaces, which accelerate drastically the flame. As a result, the locally high gradients of pressure, flow speed, and concentration of species (free radicals) are introduced within a short distance. The orifice plates create vortex structures of a size of the order of a hole. Consequently, the vortexes lead to strengthen the turbulence level (with a large spectrum of turbulence size) and the mixing between combustion products and the unreacted mixture. These mechanisms strongly increase the combustion rate and are able to generate a shock-flame system that propagates at high velocity, thus reducing the penalizing stage of flame acceleration. Therefore, the obstacle with an adapted BR will substantially reduce run-up distance and time (length of transition L_{DDT} and time τ_{DDT}).Three combinations of the obstacle configurations for the detonation chambers are tested with kerosene-air mixtures to seek the most effective DDT enhancement devices for reducing L_{DDT}.

3.1 Shchelkin spiral–orifice plates–blank tube combination ($SPDE_1$)

A schematic of $SPDE_1$ is shown in Fig. 3. A Shchelkin spirals and an orifice plate section are used as DDT devices (60 mm smooth tube in the end). The spirals, the outer diameters of which are almost equal to the inner diameter of the detonation tube, are processed using stainless steel helical compression springs. The inner diameter of the detonation tube is 29 mm and the length of the spiral section and the orifice plates section both are 300 mm. The orifice plate is processed with 2-mm-thick steel plate.

Tests are performed with the $SPDE_1$ operating in a multicycle mode at 20 and 30 Hz repetition rates. Figure 4 shows the raw pressure trace from PCB in the detonation tube end (PT6 and PT7), when SPDE is fired at 20 Hz for 0.4 s. The average peak pressures of P_6 and P_7 for all pulses are 4.51 ± 0342 and 1.89 ± 0.082 MPa, respectively. The uncertainty is calculated as the standard error on the mean with a 95 % confidence interval [21]. If other data are analyzed, there is a 95 % probability that its mean pressure would be within positive or negative standard error. The theoretical Chapman Jouguet (CJ) pressure (P_{CJ}) of gaseous kerosene–air mixtures for the equivalence ratio is approximately $16.41 \sim 20.3$ times the initial pressure (P_{CJ} in stoichiometric mixtures is shown for reference on this plot by using red dashed line). Most of the peaks of P_6 are 2.45 times the peak pressure that is usually associated with a steady CJ detonation. It is known as an overdriven detonation wave. The previous studies have indicated that the overdriven detonation wave decayed to a CJ or quasi-CJ detonation wave. The average peak pressures of P_7 are just slightly above P_{CJ}. Thus, the stable operations with periodic detonation are exhibited in the kerosene-fueled SPDE model without using additional oxygen at 20 Hz. The distance required for the overdriven detonation to successful decay into a quasi-CJ detonation is 265 mm (about $9.14d$). The similar distance is found at 30 Hz.

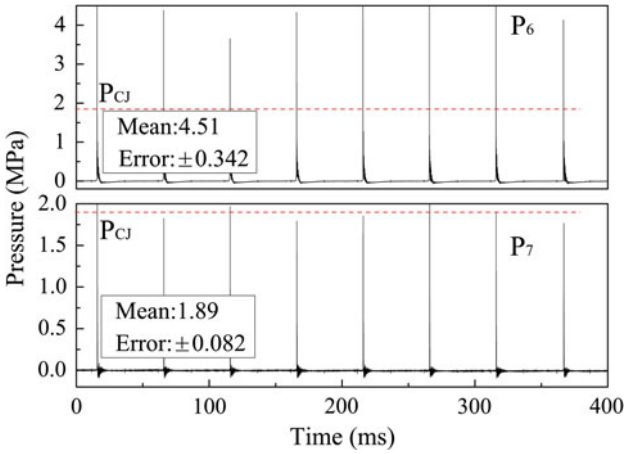

Fig. 4 Pressure time history of PT6 and PT7

The pressure and ion probe voltage profiles versus time for fifth pulse of 20 Hz are shown in Fig. 5 (Red dotted line show igniter signals), and seven measure points along the detonation tube are labeled as shown in Fig. 3. Figure 6 shows the average velocity of pressure wave and flame and maximum overpressure of the pressure wave at different propagation distances. Velocity and pressure traces are shown in Figs. 5 and 6, which provides an extra proof to support the pro-

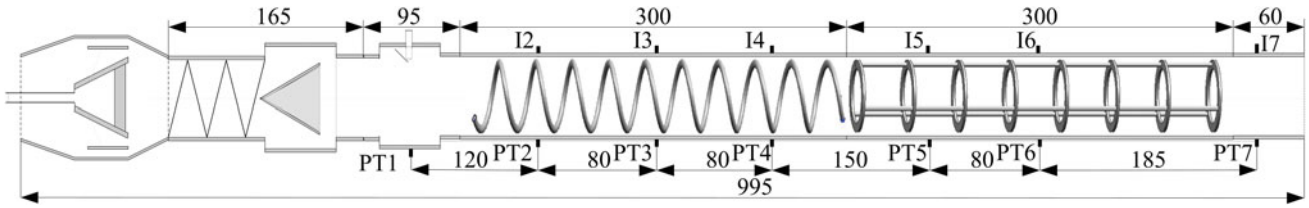

Fig. 3 Schematic of the SPDE1 (dimensions are in millimeters)

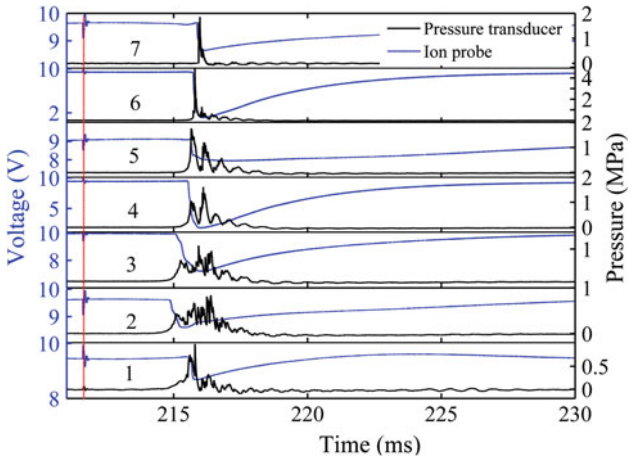

Fig. 5 Pressure profiles (*black*) and ion probe voltage profiles (*blue*) in time along the $SPDE_1$ at 20 Hz

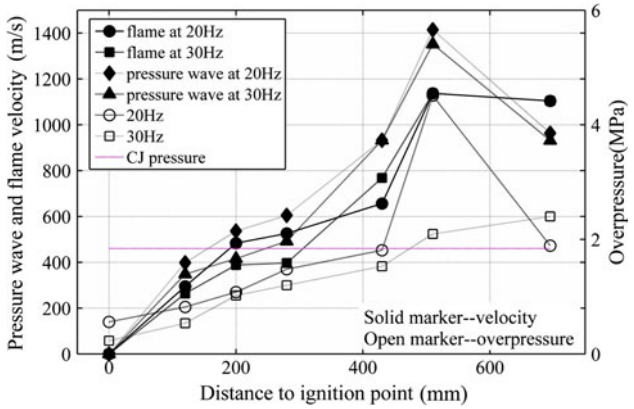

Fig. 6 Velocity (*left*) and maximum overpressure (*right*) varies with propagation distance. *Solid* marker denotes the velocity and *open marker* denotes the overpressure

posed explanation for successful detonation transition in the $SPDE_1$.

Under the weak ignition condition at 20 and 30 Hz, preheated kerosene–air mixture can be successful ignited, and the flame is accelerated during its propagation, see Figs. 5 and 6. After the ignition, the ignition section is rapidly filled with the flames. Afterwards, the fast deflagration regime is observed from the measure point 2–5, which have a characteristic separation between leading shock and flame front. The transition to detonation phase is located at the measure point 6. An approximate CJ conditions is observed at the measure point 7, as a result of decay of the overdriven detonation. Due to the positive feedback coupling among flame acceleration, turbulence fluctuation, and burning speed, the high-speed compression wave is formed ahead of the turbulent flame brush, the speed of which is close to sound speed at a distance of 120 mm from ignition point. The compression wave is strengthened with the propagating distance and finally a shock wave ahead of the flame is produced as a result of sufficiently intense combustion. A CJ deflagration wave, the velocity of which ranges from 398 to 958.3 m/s, is formed on account of the shock-flame complex systems. The obstacles help the shock-flame system to attain this high velocity and to maintain it. The reaction shock waves propagate forwards rapidly and detonation is found at the measure point 6 (PT6 or I6) as shock wave and flame front merged.

When the operating frequency is 30 Hz, the average pressure peaks are less than those of 20 Hz. This is mainly attributed to the decrease in the ignition energy and fuel-filling time as the firing frequency increase. No quasi-detonation decaying from the overdriven detonation is observed in this case.

It also can be seen from Fig. 6 that the distance of 120 mm from the igniter is the initial low-velocity flame propagation stage (compression wave with peak pressure about 0.5–0.8 Mpa is formed). From 120 to 430 mm is the high-velocity reaction leading shock stage, and the choking regime is observed in this stage (at location of 430 mm, shock Mach number is around 3 Ma and average peak pressure of shock is more than 1.53 MPa).The flame speed then remains constant for a while until it is suddenly decelerated. Further accelerations and decelerations occur, and an overdriven detonation may occur at the distance of 510 mm from the igniter, and here the peak shock and flame velocity are 1,414.4 and 1,254.4 m/s, respectively, at 20 Hz. At 30 Hz, the overdriven detonation zone evolves back to the end of the tube (A peak shock and flame velocities are 1,351.9 and 1,191.6 m/s, respectively, at location of 510 mm). The theoretical CJ velocity (v_{CJ}) of two-phase mixtures is around 1,558.6 m/s [22]. The velocity of detonation wave is less than v_{CJ}. This may be attributed to the low reactivity of the kerosene–air mixture, the loss of flow resistance from DDT devices, and higher heat dissipation rate of the small-scale tube wall. The transition stage from leading shock reaction to overdriven detonation depends more on the thermodynamically condition that is behind the leading shock than on the turbulent flame acceleration. This difference of detonation behavior at 695 mm between 20 and 30 Hz, which can be explained by the difference of the energy sustained.

3.2 Shchelkin spiral–orifice plates–shock focusing end wall combination ($SPDE_2$)

A schematic of $SPDE_2$ is shown in Fig. 7. The Shchelkin spirals, orifice plates, and shock focusing sections are used as DDT devices. The shock focusing end wall, the length and BR of which are 100 mm and about 43 %, respectively, is consisted of a cone and a plate welded together by 1.5 mm welding rod. The inner diameter of the detonation tube is 29 mm and the length of the shock focusing section is 165 mm.

Figure 8 shows the raw pressure traces from PCB in the tube end (PT5-PT7 as labeled in Fig. 7), when the $SPDE_2$

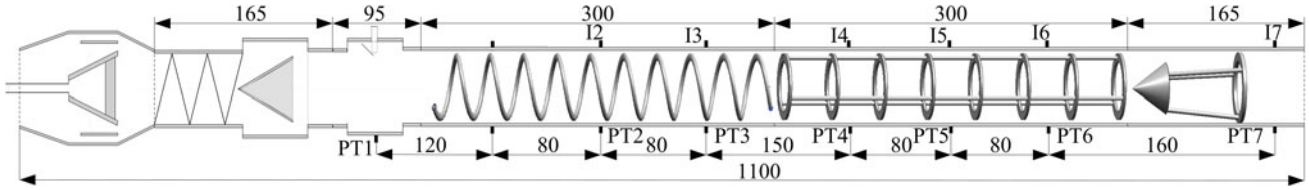

Fig. 7 Schematic of the SPDE2 (dimensions are in millimeters)

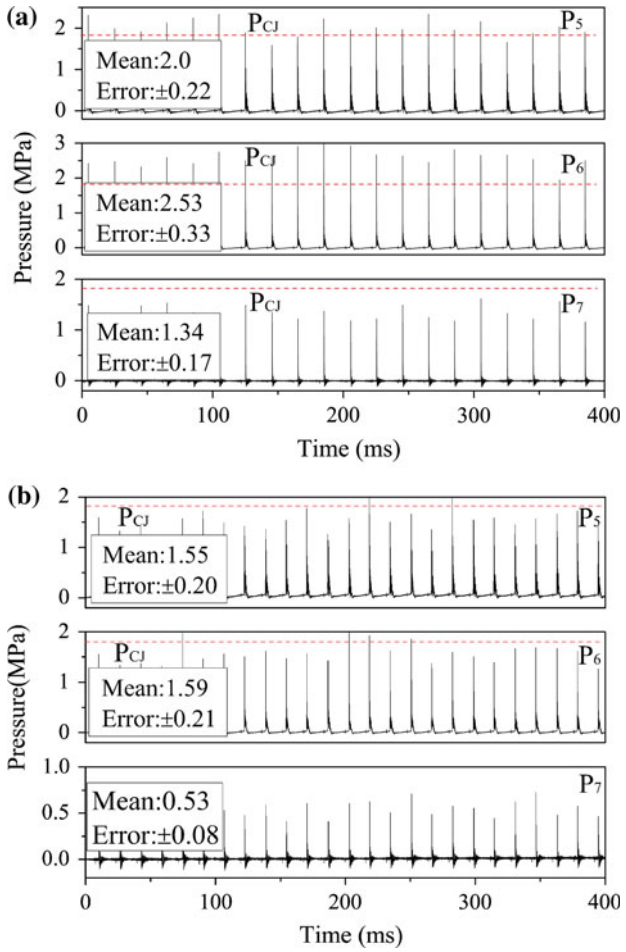

Fig. 8 Pressure time history of PT5, PT6 and PT7. **a** 50 Hz, **b** 62.5 Hz

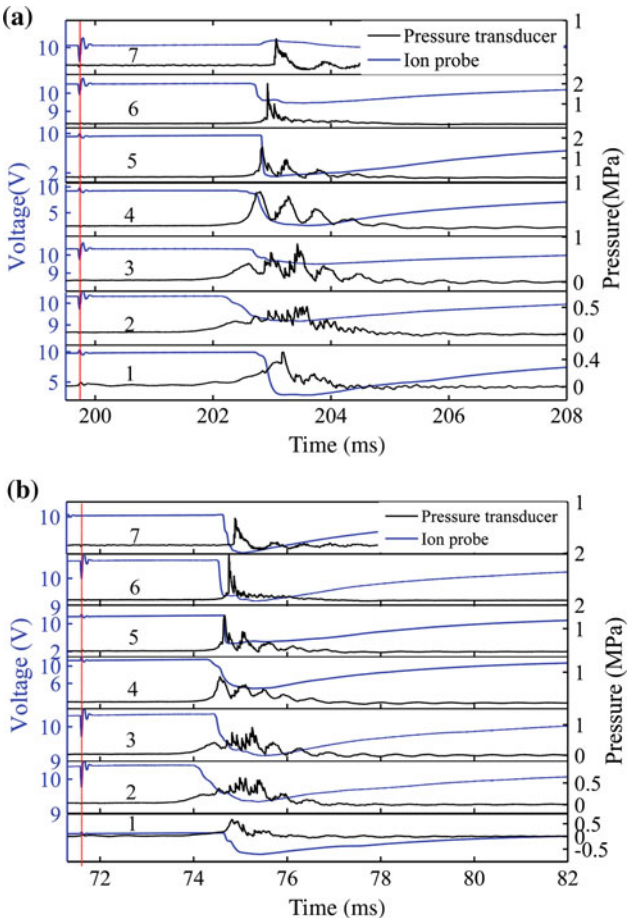

Fig. 9 Pressure profiles (*black*) and ion probe voltage profiles (*blue*) in time along the $SPDE_2$. **a** 50 Hz, **b** 62.5 Hz

was fired at the 50 and 62.5 Hz. At 50 Hz, the average peak pressure of PT5 is higher than P_{CJ}, which is identified as the occurrence of recorded overdriven detonation. Then overdriven detonation wave is strengthened at the measure point 6, and the peak pressure is 1.38 times P_{CJ}. From Fig. 9a, the burning of this mixture by overdriven detonation creates an arbitrarily high pressure shock. The formed shock coalesces with the precursor shock and flame and eventually transits to be a stable detonation. The overdriven detonation is first recorded at 240 mm (about 8.3*d*) from igniter. The successful occurrence of a quasi-CJ detonation decaying from overdriven detonation is observed at 510 mm. At 62.5 Hz, the average peak pressures along the detonation tube are less than P_{CJ}, and P_7 is equal to 0.3 P_{CJ}. Therefore, a fully developed detonation wave is not successfully triggered in the $SPDE_2$ with 62.5 Hz. The main reason is the lack of sustained energy supply due to decrease of the fired energy and the worse detonable mixed gas. However, the stable pulse combustion wave is observed and the similar traces of pressure and flame wave are shown in Figs. 8b and 9b.

Figure 10 shows the mean velocities of different measuring segments in Fig. 7. The precursor shock velocities are found to be quite close to those of the flame waves, giving

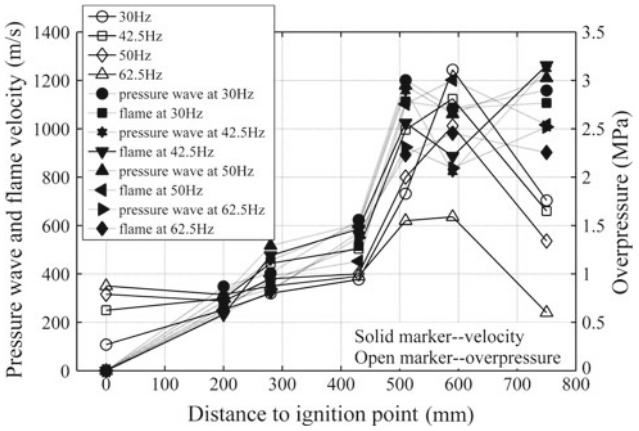

Fig. 10 Velocity (*left*) and maximum overpressure (*right*) varies with propagation distance. *Solid marker* denotes the velocity and *open marker* denotes the overpressure

the impression that the two waves are coupled and propagated as a steady reaction front-precursor shock complex like that of a stable detonation [23]. The flame velocity of the kerosene-air reaction zone is slightly slower than the velocity of the precursor shock, and this phenomenon indicates that the reaction rate is changed with time. The precursor shock and flame velocities couple at the measure point 5, and both velocities are close to the v_{CJ}. Thus, the final onsets of detonation waves are seen in the experiment and occur at a similar run-up distance that is 510 mm from igniter.

At 62.5 Hz, the mean speeds of flame and pressure wave are lower than v_{CJ}. The high-speed turbulent deflagration and precursor shock propagates approximately at a constant speed corresponding to 900 m/s (0.6 v_{CJ}), from which a detonation wave cannot be transitioned without enough energy sustaining. However, the critical conditions of the onset of detonation regime at the higher frequency cannot be readily studied, due to lack of the more details from reaction zone-shock complex of the deflagration wave.

3.3 Shchelkin spiral–two orifice plates sections combination ($SPDE_3$)

A schematic of $SPDE_3$ is shown in Fig. 11. A shchelkin spiral and two orifice plates sections are used as DDT devices. The inner diameter of the detonation tube is 29 mm and the length of the two spiral sections are 300 and 240 mm, respectively.

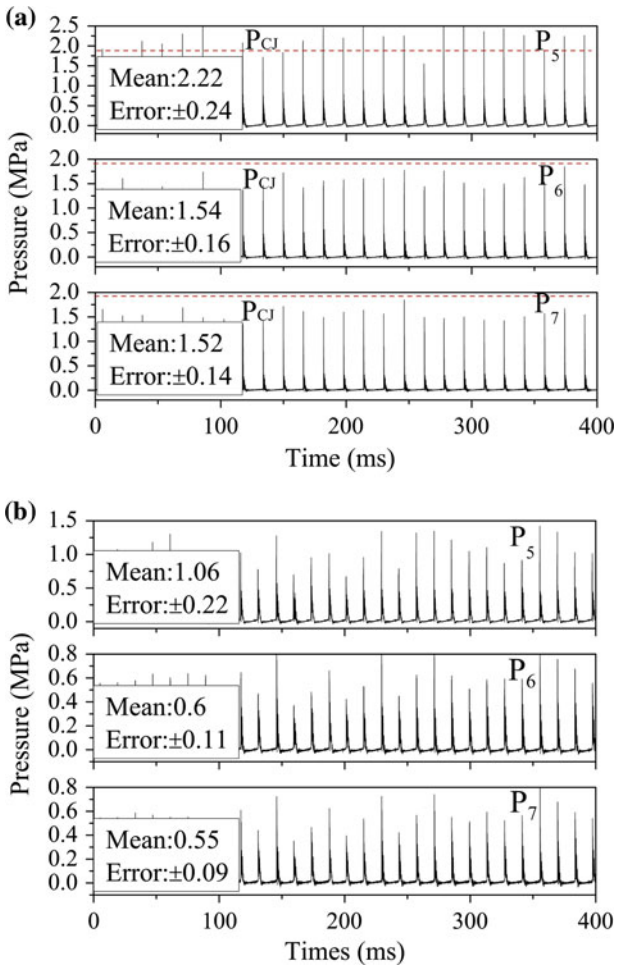

Fig. 12 Pressure time history of PT5, PT6 and PT7. **a** 62.5 Hz, **b** 71.4 Hz

Figure 12 shows the raw pressure traces along the detonation tube (PT5-PT7) when the $SPDE_3$ is fired at 62.5 and 71.4 Hz. It is seen Fig. 12a that the average peak pressure of PT5 is higher than P_{CJ} (about 1.2 P_{CJ}), and a successful transition of the quasi-CJ detonation occurs at the measure point 6. Afterwards, the pressure declines slightly at the measure point 7. At 62.5 Hz, a quasi-steady detonation wave is successfully triggered in the $SPDE_3$. The degree of the overdriven detonation wave decreases as the frequency increases. It is clearly seen that a pulse combustion wave comes up rather than a detonation at 71.4 Hz as shown in Fig. 12b. Due to the bad detonable mixed gas and fired energy decrease, the

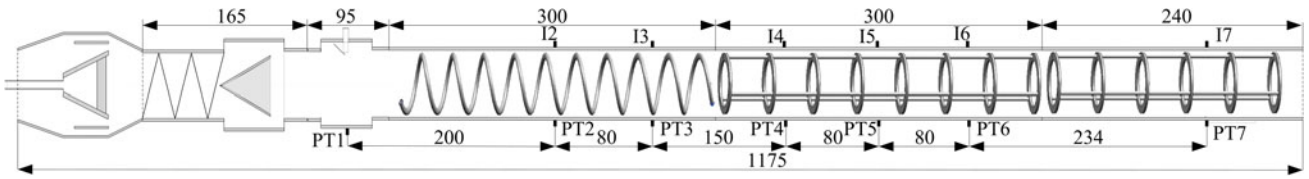

Fig. 11 Schematic of the $SPDE_3$ (dimensions are in millimeters)

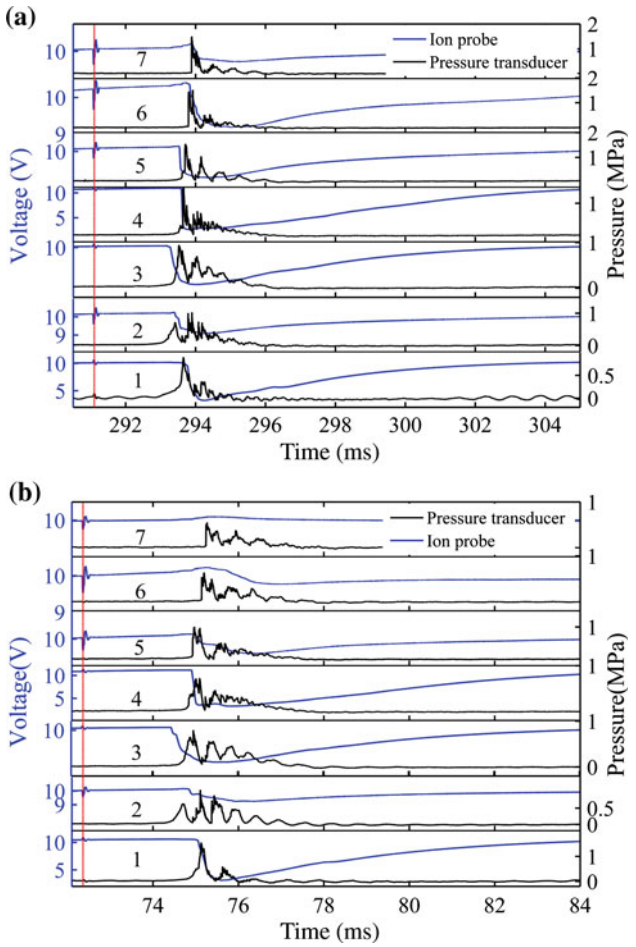

Fig. 13 Pressure profiles (*black*) and ion probe voltage profiles (*blue*) in time along the $SPDE_3$. **a** 62.5 Hz, **b** 71.4 Hz

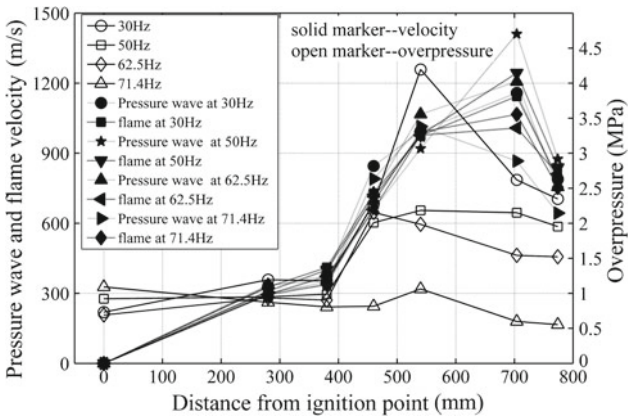

Fig. 14 Velocity (*left*) and maximum overpressure (*right*) varies with propagation distance. *Solid marker* denotes the velocity and *open marker* denotes the overpressure

high-speed deflagration wave dies off such that only a strong deflagration flame exists inside $SPDE_3$.

Figure 13 shows the pressure wave and flame traces along the detonation tube of $SPDE_3$. Figure 14 shows the mean velocities of different measuring segments (labeled as shown in Fig. 11). It is seen Fig. 13a that the flame acceleration leads to form a leading shock wave in the flow ahead, and the shock wave is finally coalesced and overlapped with flame. A slight overdriven detonation is recorded by pressure transducer PT4 and then decays to quasi-CJ detonation. Thus, the detonation transition occur at 62.5 Hz. The similar recorded traces are observed in Fig. 13b, in which a leading shock wave is generated by accelerating flame, but the high-speed deflagration wave dies off as it propagates.

Figure 14 provides additional proofs to show the successful detonation transition has already happened at 30, 50, and 62.5 Hz. The flame velocity grows exponentially so that the compression pressure waves are produced. The compression waves are strengthened to the leading strong shocks in the flow far ahead of the flame. Afterwards, the flames are accelerated to the highest value and an abrupt increase of velocity is observed as a result of the formation of a transient overdriven detonation. Eventually, the flame velocities are close to the velocities of shock waves and the overdriven detonation wave decays subsequently towards a quasi-stable detonation wave.

3.4 Detonation transitions in the multi-cycle SPDEs

These experiments confirm that the successful transitions of the detonation can be attained, and the dissimilar DDT characterizes at different frequencies are observed. The tests show that a successful detonation transition cannot be obtained when the operating frequencies are greater than 62.5 Hz, no matter what kinds of combination of obstacles are used. The air filling speeds adopted at the high frequencies (50, 62.5, and 71.4 Hz, and the filling speeds approximately equal to 120 m/s) are higher than those of low frequencies (20 and 30 Hz). The results show the successful transitions are easier obtained as the filling velocities increase. This is mainly attributed to the increase in the turbulence intensity as the mixture velocity increased. The increase of the turbulence intensity leads to an increase in flame surface and heat release rate per frontal area of wrinkled flame sheet; accordingly DDT time is shortened. In some tests with the high frequencies, failures to transition occur in the initial few cycle and the successful transitions happen subsequently. It is possible that heat of the tube wall plays a role in advancing the successful detonation transition.

The ignition delay time (τ_{delay}) is the time taken after the activation energy has been imparted to a mixture of fuel and oxidizer before the exothermic chemical reaction rate begins to increase very rapidly and energy is released in a very short duration. τ_{delay} can be calculated as the time difference between the signal of the ignition and the initiation of chemical reaction in an adjacent layer of the combustible mixture (The density of atoms and free radicals increases when the combustible mixture is ignited, which leads to ionic

Table 1 Parameters for transition to detonation

Model	f (Hz)	p_1 (MPa)	p_2 (MPa)	p_3 (MPa)	v_{shock} (m/s)	v_{flame} (m/s)	τ_{delay} (ms)	τ_{DDT} (ms)	L_{DDT} (mm)	n
$SPDE_1$	20	1.81	4.51	1.89	1,414.5	1,254.4	2.88	1.18	510	3.4
	30	1.53	N/A	N/A	1,351.9	1,191.6	3.30	1.37	510	3.4
$SPDE_2$	30	0.94	3.11	1.76	1,201	1,113	2.85	0.73	510	3.4
	42.5	1.26	2.8	1.65	1,156.4	1,024.1	2.61	0.56	510	3.4
	50	1	N/A	N/A	1,178.8	1,102.1	2.49	0.65	510	3.4
$SPDE_3$	30	2.28	4.2	2.3	1,158.4	1,143.8	2.51	0.61	510	3.4
	50	2	N/A	1.95	1,243.7	1,410.9	2.53	0.46	510	3.4
	62.5	0.9	N/A	N/A	1,206.8	1,008	2.13	0.53	510	3.4

$n = L_{DDT}/L_{ch}$
p_1 Pressure at stage from shock reaction to critical leading shock, p_2 pressure of overdriven detonation, p_3 pressure of quasi-stable detonation, v_{flame} flame velocity, v_{shock} shock wave velocity

conduction. Thus, the voltage of ion probe starts to drop). A combustion wave is initiated in the kerosene–air mixture by an electric spark. The burned gas expands and drives a flow in the kerosene–air mixture. The flow becomes highly turbulized due to the no-slip boundary condition at the wall and the geometry of the SPDEs. The high turbulized flow and turbulence distorts the flame front, increases the burning rate of fuel mixture, and leads to the flame acceleration. An accelerating flame front compresses pressure waves that heat the fuel mixture ahead of it until an explosion is triggered that eventually develops into a detonation. DDT time (τ_{DDT}) is the time from mixtures ignition to the detonation formation. The ignition delay time and the DDT time are described in detail in the work of Huang et al. [24].

The minimum characteristic distance (L_{ch}) for gaseous detonation formation in the tube with repeated obstacles is given by $L_{ch} = ((d + S)/2)/\left(1 - d'/d\right)$ [6], where d is the tube diameter, S is the obstacle spacing (here take value equal to $1.5d$), and d' is the diameter of unobstructed tube. A correlation for successful transition to detonation has been found that the characteristic channel dimension must be greater than 7 times the cell size of kerosene-air [6]. The DDT distance found in the authors' study is slightly less than 7 times the cell size. The probable reason could be inadequate length of the tube for reaching steady conditions of detonation propagation. The features for transition to detonation are obtained during the investigations and the calculated results are summarized in Table 1. As seen in Table 1, the ignition delay time of the kerosene–air mixtures in three SPDE models is 2.88–3.30, 2.49–2.85, and 2.13–2.53 ms after the start of the fuel injection. Afterwards, the $SPDE_1$, $SPDE_2$ and $SPDE_3$ need around 1.18–1.37, 0.56–0.73, and 0.46–0.61 ms from combustion wave transition to detonation, respectively. As the length of SPDE increase, DDT time decrease attributing to improvement of the fuel atomization and mixing.

L_{DDT} of kerosene–air mixtures should be significantly longer than the L_{ch}. The values of L_{DDT} in $SPDE_1$, $SPDE_2$, and $SPDE_3$ are almost 510 mm from the ignition point observed in the present study, which are 3.4-times larger than L_{ch}. In fact, as the length of detonation tube increases, the detonable mixture filling distance increases as well. In turn, this leads to a decrease in the total chemical energy of unit volume detonable mixture content per cycle, which lengthens DDT distances. As the limited number of measuring segments, no evident increase in the L_{DDT} of $SPDE_2$ and $SPDE_3$ is observed compared with $SPDE_1$. The results of L_{DDT} and τ_{delay} are less than that of the finding of Frolov et al. [13]. In all tests, the average speeds of the detonation wave equal approximately 1,000 ~ 1,400 m/s and less than v_{CJ}. These findings may be attributed to the low reactivity of the kerosene-air mixture, the loss of flow resistance from DDT devices, and higher heat dissipation rate of the small-scale tube wall. The overdriven detonation attains a maximum speed and then gradually decouples into a self-sustained detonation or sub-CJ detonation with further propagation. In fact, the mixture emits to ambient and is contaminated with air near exit, and the kerosene–air becomes the lean mixture. In turn, this leads to a decrease of energy release of combustion. Without deriving enough energy from the combustion, the steady detonation wave cannot be sustained near exit of tube.

As the firing frequency increases, the value of detonation wave pressure and velocity both show a decreasing tendency. This is mainly attributed to a decrease in the ignition energy and deterioration of the fuel atomization and mixing as firing frequency increased. When the frequencies are constant, the higher the average peak pressures of detonation, the greater the instantaneous impulses. Similarly, when the pressures of detonation wave are constant, the thrust of SPDE would increase with the frequencies. From these views of performance, each SPDE model would have an optimal frequency. This hypothesis is reinforced by a series of experiments performed at different frequencies with repeated times. As seen in Table 1 and summarization above, the optimal frequency of $SPDE_1$, $SPDE_2$, and $SPDE_3$ are 20, 42.5, and 50 Hz, respectively.

3.5 Experimental uncertainty

The main sources of uncertainty are due to the sampling rate and accuracy of the pressure transducers and ion probes used

to detect the wave arrival and quantitative parameters in the obstructed tube. First, the flame structure for acceleration process in the obstructed tube is complicated, so our ideas concerning the operation of the ion probe in a turbulent flame are only qualitative. Second, the transmission of pressure wave in the tube with the complex regimes also affects the accuracy of the pressure measurement. Last, since the data sampling rate is 2.5 MHz, the wave could even travel across the part of the transducer head before being detected.

There are different parameters in the same measuring parts at different pulses, which is due to the difference of detonation initiating condition disturbed by last pulse. However, the trajectory trends of the pressure wave and flame during the DDT process are similar. Therefore, the qualitative analysis of DDT regimes based on the multi-cycle experimental results is feasible. The short distance of measurement in the SPDE could miss the details of some transient modes, such as high-speed galloping combustion and low-velocity galloping detonation [8].However, the general process of DDT in kerosene–air mixture based on the experimental results has been revealed, which would be useful for designing liquid-fueled SPDE at high frequencies.

4 Conclusions

A series of multi-cycle tests is conducted to seek efficient DDT enhancement approaches that reduce DDT distance and time and increase the frequencies of kerosene–air SPDE. The experimental results show that with the aid of kerosene–air mixture preheating, the detonability of liquid kerosene mixture is significant improved and the fully developed detonation wave can be achieved with three different combinations of obstacles as DDT devices. The high temperature of the tube wall could play a role in advance the successful detonation transition in the SPDE models. The SPDE can steadily operate at a maximal frequency of 62.5 Hz. DDT distances of kerosene–air mixtures are significantly longer than the minimum characteristic distance for gaseous detonation formation (about 3.4 times L_{ch}). The distance required for the overdriven detonation to successful decay into a quasi-CJ detonation is about $10d$. Compared with the SPDE_1, the DDT devices of SPDE_2 and SPDE_3 are more effective in shortening DDT time and increasing the operating frequency. By adopting these DDT enhancement approaches, the detonation initiation time is reduced and the detonability of kerosene is significantly improved. Therefore, it is possible to shorten the DDT time by choosing suitable DDT approaches.

The phenomena involved in the DDT process of high-frequency SPDE are investigated. The DDT process exhibits three distinct features of the combustion wave evolution in three cases: (1) an exponential flame acceleration leads to form a leading shock wave in the flow ahead, (2) the shock wave is finally coalesced and overlapped with flame and an overdriven detonation is formed, and (3) the overdriven detonation decay to a CJ or quasi-steady detonation. The detonation velocities in experimental results are less than the theoretical CJ velocities. As the firing frequency increases, the value of detonation wave pressures and velocities both decline to some extent, as well as the degree of overdriven wave.

From the perspective of performance, the optimal frequencies of SPDE_1, SPDE_2, and SPDE_3 are 20, 42.5, and 50 Hz. The SPDE_3 could be a promising high-frequency design in practical application in some extent. However, due to more obstacles and longer length of SPDE_3, the proposed design may not obtain high specific impulse. Therefore, the main challenges in the high-frequency SPDE are to ensure less loss and faster DDT rather than more obstacles for successful detonation transition, and to increase the performance by optimizing DDT enhancement techniques. Consequently, the result is a good reference for designing the suitable DDT approaches for SPDE and understanding its DDT processes in kerosene-air mixtures.

Acknowledgments This research was supported by National Natural Science Foundation of China (50776045) and Graduate Research and Innovation Fund of Jiangsu Province (CX09B_078Z). The first author would like to thank Dr. K.J. Hsieh in University of Waterloo and Dr. Jim Kuo in University of Toronto for their helps in English writing and proof reading.

References

1. Wu, Y.H., Ma, F.H., Yang, V.: System performance and thermodynamic cycle analysis of airbreathing pulse detonation engines. J. Propul. Power **19**(4), 556–567 (2003)
2. McManus, K.R., Furlong, E.R., Leyva, I.A., Sanderson, S.R.: MEMS-Based Pulse Detonation Engine for Small-Scale Propulsion Applications. In: 37th AIAA/ASME/SAE/ASEE Joint Propulsion Conference and Exhibit. AIAA 2001-34698 (2001)
3. Kitano, S., Kimura, Y., Sato, H., Hayashi, A.K.: Micro-Size pulse detonation engine performance. In: 45th AIAA Aerospace Sciences Meeting and Exhibit. AIAA 2007-581 (2007)
4. Huang, Y., Tang, H., Li, J., Wang, J.: Experimental investigation on small-scale pulse detonation engine with kerosene/air. Acta Aeronautica et Astronautica Sinica **30**(11), 2015–2022 (2011, in Chinese)
5. Valiev D., Bychkova V., Akkerman V., Eriksson L.E., Marklund M.: Heating of the fuel mixture due to viscous stress ahead of accelerating flames in deflagration-to-detonation transition. Phys. Lett. A **372**, 4850–4857 (2008)
6. Ciccarelli, G., Dorofeev, S.: Flame acceleration and transition to detonation in ducts. Prog. Energy Combust. Sci. **34**, 499–550 (2008)
7. Smirnov, N.N., Nikitin, V.F., Alyari Shurekhdeli, S.: Investigation of self-sustaining waves in metastable systems: deflagration-to-detonation transition. J. Propul. Power **25**(2), 593–608 (2009)

8. Smirnov, N.N., Nikitin, V.F., Phylippov, Y.G.: Deflagration-to-detonation transition in gases in tubes with cavities. J. Eng. Phys. Thermophys **83**(6), 1287–1316 (2010)
9. Brailovsky, I., Sivashinsky, G.I.: Hydraulic resistance as a mechanism for deflagration to detonation transition. Combust. Flame **122**, 492–499 (2000)
10. Smirnov, N.N., Boichenko, A.P.: Deflagration to detonation transition in gasoline-air mixtures. Combust. Explo. Shock. **22**(2), 65–68 (1986)
11. Smirnov, N.N., Nikitin, V.F., Boichenko, A.P., Tyurnikov, M.V., Baskakov, V.V.: Deflagration to detonation transition in gases and its application to pulse detonation devices. In: Roy, G.D., Frolov, S., Kailasanath, K., Smirnov, N. (eds.) Gaseous and Heterogeneous Detonations: Science to Applications, pp. 65–94. ENAS Publishers, Moscow (1999)
12. Smirnov, N.N., Nikitin, V.F., Khadem, J., Alyari Shourekhdeli, S.: Onset of detonation in polydispersed fuel–air mixtures. Proc. Combust. Inst. **31**, 2195–2204 (2007)
13. Roy, G.D., Frolov, S.M., Borisovb, A.A., Netzerc, D.W.: Pulse detonation propulsion challenges, current status and future perspective. Prog. Energy Combust. Sci. **30**, 545–672 (2004)
14. Teodorczyk, A., Drobniak, P., Dabkowski, A.: Fast turbulent deflagration and DDT of hydrogen–air mixtures in small obstructed channel. Int. J. Hydrogen Energy **34**, 5887–5893 (2009)
15. Sorin, R., Zitoun, R., Desbordes, D.: Optimization of the deflagration to detonation transition: reduction of length and time of transition. Shock Waves **15**(2), 137–145 (2006)
16. Frolov, S.M., Basevich, V.Y., Aksenov, V.S.: Optimization study of spray detonation initiation by electric discharges. Shock Waves **14**(3), 175–186 (1999)
17. Frolov, S.M., Aksenov, V.S.: Deflagration to detonation transition in kerosene–air mixture. Dokl. Phys. Chem. **416**(3), 356–359 (2007)
18. Frolov, S.M.: Liquid-fueled, air-breathing pulse detonation engine demonstrator: operation principles and performance. J. Propul. Power **22**(6), 1162–1169 (2006)
19. Shchelkin, K.I., Troshin, Y.K.: Gas Dynamics of Combustion. USSR Acad. Sci. Publ., Moscow (1963)
20. Tang, H., Huang, Y., Li J., Wang, J.: Mechanism Research of Small-scale Pulse Detonation Engine. In: Proceedings of 1st symposium on detonation and detonation engine in China (2009)
21. Rasheed, A., Furman, A.H., Dean, A.J.: Pressure measurements and attenuation in a hybrid multitube pulse detonation turbine system. J. Propul. Power **25**(1), 148–161 (2009)
22. Nicholls, A., Sichel, M., Fry, R.S., Hu, C., Glass, D.R., DeSaro, K., Kearney, K.: Fundamental aspects of unconfined explosions. Technical Report AFATL -TR-73-125 (1973)
23. Zhu, Y.J., Chao, J., Otsuka, T., Lee, J.H.S.: An experimental investigation of the propagation mechanism of critical deflagration waves that lead to the onset of detonation. Proc. Combust. Inst **31**(2), 2455–2462 (2007)
24. Huang, Y., Tang, H., Li, J., Zhang, C.: Experimental Investigation on Two Phases Small-scale Pulse Detonation Engine at the high frequency. In: Proceedings 3rd International Symposium on Jet Propulsion and Power Engineering. 2010-ISJPPE-5019 (2010)